New type of electric oscillations in bistable resonant tunneling diodes

B. A. Glavin and V. A. Kochelap[a)]
Institute of Semiconductor Physics, Pr. Nauki 45, Kiev 252028, Ukraine

V. V. Mitin
Department of ECE, Wayne State University, Detroit, Michigan 48202

(Received 28 September 1998; accepted 8 December 1998)

We studied a resonant tunneling diode with intrinsic bistability when high and low current states simultaneously occur in a certain voltage range. We have found a novel type of electric oscillation in the bistable resonant tunneling diode. Under these oscillations one portion of the diode is in the high current state while the other is in the low current state. A periodic motion of the boundary between the high and low current regions gives rise to oscillations of the current in the external circuit. © *1999 American Institute of Physics.* [S0021-8979(99)01206-2]

I. INTRODUCTION

The intrinsic bistability of the resonant tunneling diodes (RTDs) is an extensively studied phenomenon since its first observation.[1] The physical reason of the bistability is an accumulation of the resonant electrons in the quantum well, i.e., a charge built up between the barriers. Indeed, when the voltage bias shifts the resonant level below the bottom of the emitter conduction band, the built-up charge pushes this resonant level up and can regain the resonant tunneling conditions. This gives rise to the existence of two current states, low and high, in the diode at a given voltage bias. Under such conditions a negative differential resistance is minimum, and the current–voltage characteristic has the bistability of *Z* type.

Recently we reported that in bistable RTDs transverse patterns can occur spontaneously.[2] These patterns are nonuniform distributions of the built-up charge in the quantum well layer and nonuniform tunneling current. Among different types of the patterns, mobile switching waves (SWs) have been discovered. They correspond to a switching of the diode from one transversely uniform state to another. The front of a SW can be characterized by the width, $L_D \sim v_F \tau_{ch}$. The quantities v_F, τ_{ch}, are the Fermi velocity of electrons injected into the well and the characteristic time of their escape from the well, respectively. The velocity of a SW, v, is of the order of v_F and depends on the voltage applied to the diode, Φ. Within the bistable voltage range $\Phi_l < \Phi < \Phi_h$, as shown schematically in Fig. 1(a), a critical voltage Φ_c exists that corresponds to the stationary kink-like pattern. This pattern is the transient region between the high and low current states. At $\Phi_l < \Phi < \Phi_c$ SWs perform switching from the low current state to the high current state. At $\Phi_c < \Phi < \Phi_h$ the reverse switching is possible.

We have shown that SWs can be induced by nonuniformities within the quantum well or barrier layers. To induce switching from the low current state to that of the high current, the nonuniformity should provide an additional injection of electrons from the emitter to the quantum well. Moreover, to induce switching from the high current state to that of the low current, the nonuniformity should behave as a drain for the resonant electrons. Consequently, the switching produced is due to the leakage of the resonant electrons along the quantum well layer away from the nonuniformity. As a result, the low current branch of the RTD current–voltage characteristic at $\Phi_l < \Phi < \Phi_c$ and the high current branch at $\Phi_c < \Phi < \Phi_h$ can become unstable with respect to the spontaneous SW inducement.

Particularly, such nonuniformities can be formed near the edges of the heterostructure. For example, they arise due to a depletion layer at the sample surface and due to a variation of the quantum well and barrier layers thicknesses, etc. In such an example, we can refer to the article[3] which stated the influence of the depletion layer on the properties of the RTD as observed experimentally in the case of the high and low charge accumulation in the quantum well. Therefore, an additional source or drain of resonant electrons can be provided by the means of additional electrodes (see, for example Ref. 4).

If the voltage bias of the RTD is constant, the inducement of a SW leads to the complete switching of the device. In fact, the RTD is always coupled with an external circuit. Since the switching is accompanied by a change of the current, the reaction of the circuit changes the voltage bias of the RTD and, consequently, the velocity of the SW. As we will show below, this feedback gives rise to the complex dynamics of the whole system consisting of the RTD and circuit. Particularly, in such a system the SW can slow down and, then, change the direction of propagation and return the RTD to the initial uniform state. Moreover, such coupling of the RTD and resonance circuit can give rise to the oscillatory behavior of the system.

II. MODEL AND BASIC EQUATIONS

We consider the simple circuit as depicted in Fig. 1(b). It consists of a RTD, a resistance R, and a resonance circuit with capacitance C and inductance L^*. To be specific, we will present results for this circuit with an unstable high current branch at $\Phi_c < \Phi < \Phi_h$ with respect to the SW induce-

a)Electronic mail: nika@div1.semicond.kiev.ua

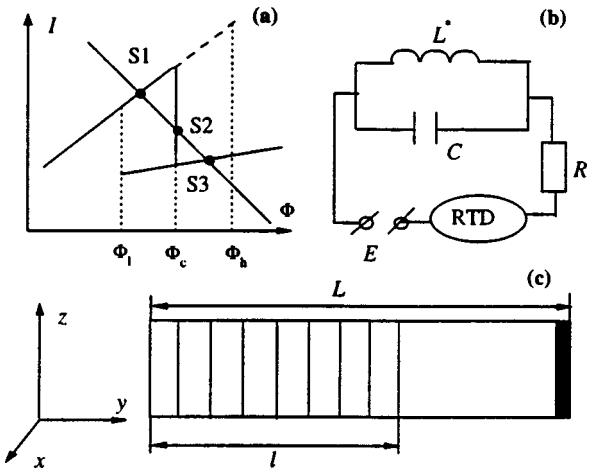

FIG. 1. (a) A sketch of the current–voltage characteristic of a bistable RTD. The load line is shown by the dashed line and stationary states of the system are marked by $S1$, $S2$, and $S3$. (b) The electric circuit under consideration; it consists of the resonance circuit, the RTD and the series resistance R. (c) A schematic cross-section of an RTD. The portion of the RTD of length l is in the high current state (dashed area) while the portion of length $L-l$ is in the low current state. At $y=L$ the edge nonuniformity can induce SWs.

ment. Qualitatively the same results can be obtained for a RTD with unstable low current branch at $\Phi_l<\Phi<\Phi_c$.

The cross-section of the RTD transverse to the current in the quantum well region is schematically presented in Fig. 1(c). We assume that the cross-section is rectangular with dimensions, L and h, along the y and z axes, respectively. The current flows along the x axis. In addition, we assume that the SW can be induced by an additional drain for the resonant electrons within the edge of the structure at $y=L$. Such a simple geometry of the device provides a one-dimensional character of the SW, which in this case propagates along the y direction. We suppose that the SW width, L_D, is much less than the diode dimension, L. Next, we denote the dimension of the portion of the RTD in the high current state as l. This portion is shown as the shaded region $0<y<l$ in Fig. 1(c), while the rest of the RTD, $l<y<L$, is in the low current state.

Stationary states of the system are determined by intersections of the RTD current–voltage characteristic and load line as shown in Fig. 1(a). We assume that the load line crosses the high current branch of the RTD current–voltage characteristic at $\Phi_l<\Phi<\Phi_c$ and at the low current branch at $\Phi_c<\Phi<\Phi_h$. Two possible stationary states $S1$ and $S3$ correspond to the uniform high and low current states, respectively. The third stationary state, $S2$, corresponds to the kink-like state with $\Phi=\Phi_c$. Obviously, the states $S1$ and $S3$ are stable with respect to the small perturbations while the state $S2$ is unstable. However, the state $S1$ is unstable with respect to the large perturbations, $\Delta\Phi>\Phi_c-\Phi$, since such perturbations lead to the appearance of a SW.

In Fig. 2 we present the possible types of the temporal evolution of the voltage bias, Φ, and the dimension of the high current region, l, after the SW inducement at the moment $t=0$. Depending on parameters of the RTD and circuit three types of the evolution are possible. Figure 2(a) corresponds to parameters of the system, when the complete

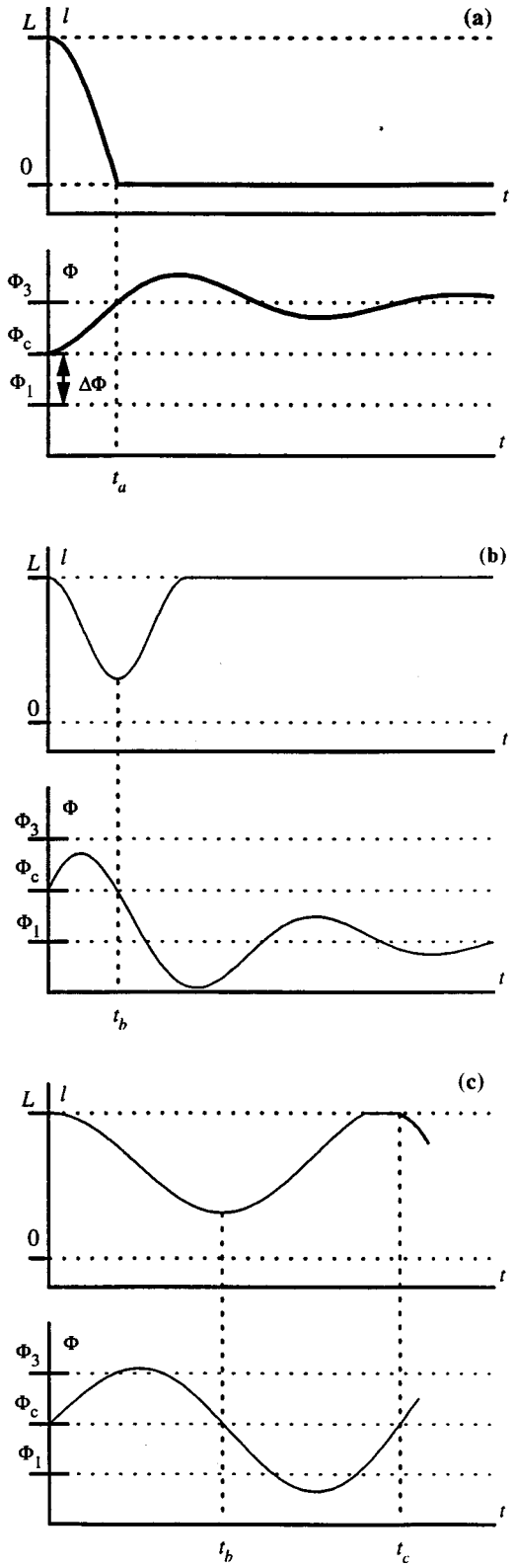

FIG. 2. Possible types of temporal evolution of values, l and Φ: (a) Inducement of the switching wave results in the complete switching of the diode; (b) inducement of the SW leads to the return of the system into the initial uniform high current state; (c) the RTD returns to the high current uniform state, and the switching wave is induced again.

switching of the diode from the high to low current uniform state occurs during the time interval t_a. In this case the voltage bias, Φ, is always greater than Φ_c, and the SW does not change the direction of propagation. After the diode is

switched, the circuit behaves as a damped oscillator, and Φ approaches the value, Φ_3. Figures 2(b) and 2(c) correspond to the system parameters when at some time, t_b, the voltage, Φ, becomes less than Φ_c. Next, the SW reverses its direction of motion, and the RTD returns to the uniform high current state. Then, the circuit behaves as a damped oscillator. If Φ is always less than Φ_c, then the system is in the state, $S1$, as shown in Fig. 2(b). Alternatively, if at time, t_c, the voltage Φ becomes greater than Φ_c, the SW is induced again, as shown in Fig. 2(c). Obviously, if at a time, t_c, the system is returned into the state which coincides *exactly* with the initial state, the evolution is periodic. Next, we will analyze how the temporal evolution of the system depends on the parameters of the RTD and circuit.

We shall consider the dynamics of a RTD in the quasistationary approach when the instant velocity of the SW, $v(t)$, can be assumed to be dependent on the instant value of the voltage bias, $\Phi(t)$. This assumption is valid if the eigen frequency of the circuit, $\omega_0 \equiv (L^*C)^{-1/2}$, is much less then inverse times of intrinsic processes within the RTD. The RTD intrinsic times include: the time of tunneling escape of the resonant electrons from the quantum well and the time of the discharge of the RTD intrinsic capacitance.[5] The dependence $v(\Phi)$ is obtained from different approaches.[2] In evaluating the current, we shall neglect the current contribution from the transition region between the low and high current states because of $L \gg L_D$.

As shown in Fig. 2, all possible cycles of the dynamics of the system consist of two different stages. During the first stage, a SW propagates through the RTD, and during the second stage, the RTD is in the uniform high current state. For the first stage with SW propagation, the current through the RTD is determined by the equation

$$I(t) = \frac{l}{L} I^{(h)}[\Phi(t)] + \left(1 - \frac{l}{L}\right) I^{(l)}[\Phi(t)], \tag{1}$$

and the dimension of the high current region of the RTD, l, obeys the equation

$$\frac{dl}{dt} = -v(\Phi) = -\beta(\Phi - \Phi_c). \tag{2}$$

Here $I^{(h)}(\Phi)$ and $I^{(l)}(\Phi)$ denote the characteristics of high and low current branches of the RTD in the uniform state, respectively, and for $v(\Phi)$ near $\Phi = \Phi_c$, we introduce the linear expansion with respect to $\Phi - \Phi_c$. The accuracy of the latter approach is supported by the results of article[2] where it has been found that the dependence $v(\Phi)$ is linear almost everywhere except at narrow regions of the voltage biases close to the boundaries of the bistability region with $\Phi \approx \Phi_l$ or $\Phi \approx \Phi_h$. In calculations we assume $I^{(h)}(\Phi)$ and $I^{(l)}(\Phi)$ are linear functions of Φ near $\Phi = \Phi_c$:

$$I^{(h)}(\Phi) = I_0^{(h)} + \frac{1}{R_h}(\Phi - \Phi_c), \tag{3}$$

$$I^{(l)}(\Phi) = I_0^{(l)} + \frac{1}{R_l}(\Phi - \Phi_c). \tag{4}$$

The circuit dynamics is described by electric circuit equations,

$$\frac{d^2U}{dt^2} + \omega_0^2 U = \frac{1}{C}\frac{dI}{dt}, \tag{5}$$

$$U + IR + \Phi = E. \tag{6}$$

Here, U is the voltage drop on the resonance circuit and E is the voltage supply.

For a cycle with a SW during the first stage, the system of differential Eqs. (2) and (5) are of the third order. During the second stage of a cycle when the RTD is entirely in the high current state, this condition is described by Eq. (1) with $l = L$ and by Eqs. (5) and (6). Thus, to determine a dynamic cycle completely, three initial conditions are necessary. At the start of a cycle, two of the three initial conditions are always the same: $l = L$ (since initially the RTD is in the high current state) and $U = U_0 = E - \Phi_c - I_0^{(h)}R$. The latter is necessary to provide the condition $\Phi = \Phi_c$. The third initial condition is described by the value, $dU/dt|_{t=0} \equiv u'$ with $u' < 0$. Furthermore, for all future cycles the latter value has to be determined as a function of its value on the previous cycle. This reduces the study of complete dynamics of the system to the *one-dimensional discrete map*, $u'_k = f(u'_{k-1})$, where the index corresponds to the number of the cycle.

It can be easy shown that the system of Eqs. (1)–(6) contains the five dimensionless parameters. Three parameters describe the diode: $r_h = R_h/R$, $r_l = R_l/R$ and $\xi_c = l_c/L$ with l_c corresponding to the value of l in the stationary kink-like state, $S2$. The fourth parameter is the quality factor of the circuit: $Q = \omega_0 RC$. And the fifth parameter, $\alpha = \beta(I_0^{(h)} - I_0^{(l)})R/L\omega_0$, can be considered as the diode-circuit coupling. It can be estimated as

$$\alpha \sim \frac{2\pi}{\omega_0 \tau_{\rm sw}} \times \frac{(I_0^{(h)} - I_0^{(l)})R}{\Phi_h - \Phi_l}, \tag{7}$$

where $\tau_{\rm sw} = L/v_{\rm ch}$ is the time of the RTD switching with a characteristic switching velocity, $v_{\rm ch}$. At this point it is convenient to introduce the dimensionless value,

$$x = -\frac{1}{\omega_0 U_0}\frac{dU}{dt}\bigg|_{t=0} > 0. \tag{8}$$

Now, the evolution of the system is determined by the map: $x_k = P(x_{k-1})$. The theory of one-dimensional mapping can be found in the Ref. 6.

We have solved Eqs. (3)–(6) for different realistic parameters of the diodes and circuits. Possible types of the mapping functions, $P(x)$, are presented in Fig. 3. The parameters, α, r_h, r_l, Q, and ξ_c used in calculations are given in Table I. The straight line, $P = x$, is shown by the dashed lines. According to the theory of mapping, the *stationary points of the map*, x_{st}, are determined by the equation, $P(x_{\rm st}) = x_{\rm st}$. As discussed above, a stationary point corresponds to ordinary oscillations. They are either stable or unstable.[6] The condition of the stability at a stationary point, x_{st}, with stable oscillations is $|P'(x_{st})| < 1$.

III. MAIN TYPES OF THE SYSTEM EVOLUTION

Considering the general features of obtained dependences of the mapping functions, $P(x)$, then for any combi-

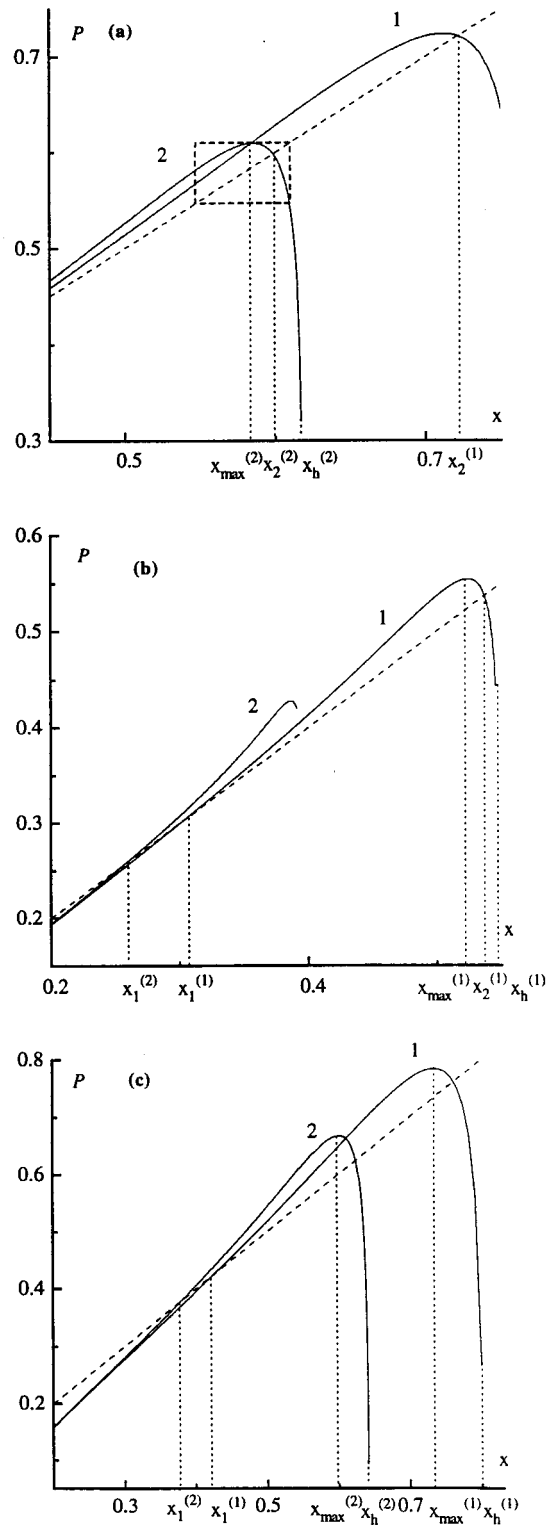

FIG. 3. Possible types of one-dimensional maps $P(x)$ for parameters of the system presented in Table I.

nation of the parameters, the functions $P(x)$ exist only for x less than specific value, x_h. At $x>x_h$ the RTD always switches to the low current state, and no further cycles exist as shown in Fig. 2(a). Then, at small x two types of the behavior of $P(x)$ are possible. In the first type $P(x)$ does not exist at small x at all, or $P(0)=0$ with $P'(0)<1$ ($x=0$ is the stable stationary point). The former means that the evolution of the system during the second stage does not lead to the following inducement of a SW. For the first type of $P(x)$ a weak perturbation of the system decays, and the system returns to $S1$. This corresponds to the temporal evolution shown in Fig. 2(b). The second type of the behavior of $P(x)$ requires conditions: $P(0)=0$ and $P'(0)>1$. This type occurs at high resistances, r_h and r_l, when dissipation in the system is practically absent during the second stage of a cycle. In this situation $x=0$ is the unstable stationary point of the map; even for small initial values of x the system does not return to the initial state, $S1$. Results for $r_h, r_l \to \infty$ have been briefly reported in Ref. 7.

TABLE I. Dimensionless parameters of the system, for which one-dimensional maps are presented in Fig. 3.

P	α	r_h	r_l	Q	ξ_c
Fig. 3(a), curve 1	1.3	100	1000	20	0.9
Fig. 3(a), curve 2	1.6	100	1000	20	0.9
Fig. 3(b), curve 1	1.8	100	1000	20	0.4
Fig. 3(b), curve 2	2.5	100	1000	20	0.1
Fig. 3(c), curve 1	1.2	50	1000	8	0.9
Fig. 3(c), curve 2	1.5	50	1000	8	0.9

In this article we have dealt with the more realistic first type of behavior of $P(x)$. All $P(x)$ dependences presented in Fig. 3 just correspond to such a case (the region of small x is not shown in the figure). The values x, for which $P(x)$ is presented, correspond to the temporal evolution of the system illustrated in Fig. 2(c).

Figure 3(a) depicts a system with $P(x)$ dependences that can demonstrate oscillatory behavior. For both curves, $P_1(x)$ and $P_2(x)$, there are two stationary points, $x_1^{(1)}$, $x_2^{(1)}$ and $x_1^{(2)}$, $x_2^{(2)}$, respectively. The points $x_1^{(1)}$ and $x_1^{(2)}$ are unstable, because $P'_{1,2}(x_1^{(1,2)})>1$. For the curve $P_1(x)$ the second stationary point is stable, $|P'_1(x_2^{(1)})|<1$. This corresponds to regular oscillations of the system. For $P_2(x)$ the second stationary point is unstable, $|P'_2(x_2^{(2)})|>1$. However, it is easy to see that there is a region of attraction marked by the dashed rectangular. Once the system exists inside this region, it never leaves it. This property holds because $P_2(x_{\max}^{(2)}) < x_h^{(2)}$, where $x_{\max}^{(2)}$ corresponds to the maximum of $P_2(x)$. Thus, both cases, $P_1(x)$ and $P_2(x)$ can provide oscillations in the system. Since $x_2^{(2)}$ is an unstable stationary point for the mapping function, $P_2(x)$, a doubling of the period of oscillations and a transition to chaotic oscillations can take place (see Ref. 6). It is important to mention that to generate such oscillations the initial value of x, x_i, should be greater than the first unstable stationary point, $x_i>x_1^{(1,2)}$; otherwise, the system returns to the initial state $S1$.

In Fig. 3(b) other $P(x)$ dependences are presented. For the curve $P_1(x)$ two stationary points exist, but the second one is unstable: $|P'_1(x_2^{(1)})|>1$. In a distinction from the curve P_2 in Fig. 3(a), there is the curve, $P_1(x_{\max}^{(1)})>x_h^{(1)}$ without a region of attraction. For $P(x)$ dependences of such a type at $x_i<x_1^{(1)}$, the system returns to the state $S1$. If $x_i>x_1^{(1)}$, the situation is more complex; the system can either latch to the oscillatory cycle similar to that of the curve $P_2(x)$ in Fig.

3(a) or switch to the state $S3$. For the curve $P_2(x)$ only one stationary point, $x_1^{(2)}$, exists. For such a $P(x)$ dependence the system either goes to the state, $S1$ (for $x_i<x_1^{(2)}$) or to the state, $S3$ (for $x_i>x_1^{(2)}$).

In Fig. 3(c) the next two variants of $P(x)$ dependences are presented. For $P_1(x)$ there are $P_1(x_h^{(1)})<x_1^{(1)}$ and $P_1(x_{\max}^{(1)})<x_h^{(1)}$. For such a mapping function at $x_i>x_1^{(1)}$, the system can either oscillate or can switch to the state, $S3$. For $P_2(x)$ the situation is even more complex. In a distinction from the case of $P_1(x)$ dependence presented in Fig. 3(b), there is $P_2(x_h^{(2)})<x_1^{(2)}$. As a result, the system can be either latched to the oscillatory cycle [similarly to that of the curve, $P_2(x)$, in Fig. 3(a)] or switch to the state, $S3$. And if $x_i>x_1^{(2)}$, a third possibility appears: the system can return to the state, $S1$.

Thus, the calculations of functions, $P(x)$, and the mapping analysis show that the system of Eqs. (1)–(6) depending on the value of parameters has different solutions: periodic solutions, oscillations with a period doubling, damped and over-damped oscillations, chaotic oscillations, etc. Every solution corresponds to a complex evolution of the circuit and spatiotemporal dynamics of the RTD. The latter includes nonuniform tunneling, leakage of electrons over the quantum well layer, nonuniform current, and more.

IV. CONCLUSIONS

It is useful to compare these results with the dynamics of conventional RTDs demonstrating the *N*-type behavior of the current–voltage characteristic. For the latter case the RTD operates as a *discrete* nonlinear element in the circuit and only a temporal evolution occurs. In the case under consideration, the RTD is accounted as the distributed object with the *Z* type of the current–voltage characteristic, where spatiotemporal transverse patterns arise and are supported by consistent temporal evolution of electrical signals in the resonant circuit. Note, the considered effect is related to the problem of stability of the *Z*-type current–voltage characteristic.[8]

In conclusion, we have demonstrated that a bistable RTD coupled with a resonance circuit can exhibit interesting behavior, including a new type of electrical oscillations and different types of switching modes.

ACKNOWLEDGMENTS

This work was supported by the Ukrainian State Committee for Science and Technology. B.G. is also grateful to Wayne State University for its support of his visit and work there. In addition, we appreciate the editing of this paper by David Cole, a graduate student at Wayne State University.

[1] V. J. Goldman, D. C. Tsui, J. E. Cunningham, Phys. Rev. Lett. **58**, 1256 (1987).
[2] V. A. Kochelap, B. A. Glavin, and V. V. Mitin, Phys. Rev. B **56**, 13346 (1997).
[3] T. Schmidt, M. Tewordt, R. J. Haug, K. von Klitzing, B. Schönherr, P. Grambow, A. Förster, and H. Lüth, Appl. Phys. Lett. **68**, 838 (1996).
[4] P. H. Beton, M. W. Dellow, P. C. Main, T. J. Foster, L. Eaves, A. F. Jezierski, M. Henini, S. P. Beaumont, and C. D. W. Wilkinson, Appl. Phys. Lett. **60**, 2508 (1992).
[5] T. C. L. G. Sollner, E. R. Brown, J. R. Söderström, T. C. McGill, C. D. Parker, and W. D. Goodhue, in *Resonant Tunneling in Semiconductors: Physics and Applications*, edited by L. L. Chang, E. E. Mendez, and C. Tejedor (Plenum, New York, 1990), p. 487.
[6] G. Schuster, *Deterministic Chaos: An Introduction* (VCH, Weinheim, 1995).
[7] B. A. Glavin, V. A. Kochelap, and V. V. Mitin, in *Proceedings of the International Conference on Quantum Devices and Circuits*, edited by K. Ismail, S. Bandyopadhay, and J.-P. Leburton (Imperial College Press, 1996), p. 170.
[8] A. Wacker and E. Schöll, J. Appl. Phys. **78**, 7352 (1995).